Journal of Alloys and Compounds 509 (2011) 6946–6949

Contents lists available at ScienceDirect

Journal of Alloys and Compounds

journal homepage: www.elsevier.com/locate/jallcom

Magnetic properties of Al_2O_3–Cr_2O_3 solid solutions

S.H. Yang[a], S.J. Liu[b], Z.H. Hua[a], S.G. Yang[a,*]

[a] National Laboratory of Microstructure and Department of Physics, Nanjing University, Nanjing 210093, China
[b] College of Physics and Electronic Information, Luoyang Normal College, Luoyang 471022, China

ARTICLE INFO

Article history:
Received 27 December 2010
Received in revised form 1 April 2011
Accepted 1 April 2011
Available online 8 April 2011

Keywords:
Solid solution
Cr_2O_3
Néel temperature
SQUID
XRD

ABSTRACT

Solid solution ceramics $(Al_2O_3)_x(Cr_2O_3)_{1-x}$ with different x in the range of $0<x<1$ were synthesized via traditional ceramic production method. X-ray diffraction results and Rietveld refinements indicated that all samples possessed rhomb-centered structure and continuous solid solutions were synthesized. The samples were composed of irregular grains with several micrometers in diameter. Temperature dependence of magnetization measurements showed monotonous decreasing Néel temperature with increasing x and percolation effect happened with threshold of $x=0.65$. As x became higher, weak ferromagnetism was observed in the samples. Field dependence of magnetization measurements further confirmed the weak ferromagnetism in the samples with $x=0.7$, 0.8 and 0.9.

1. Introduction

Antiferromagnetic (AFM) materials are a kind of the most important ordered magnetic materials not only for fundamental physics but also for applications, such as the production of high-recording-density hard disks based on giant-magnetoresistive effect [1], enhancement of coercivity of magnet based on pinning effect, beating of superparamagnetic (SPM) limit [2], and high sensitive spin valve devices [3,4] based on the exchange bias effect [2,5]. Thus the properties of the AFM materials are an interesting and important research topic. Magnetic phase transition temperature between AFM and paramagnetism (PM), so-called Néel temperature (T_N), is the most important characteristic parameter of the AFM materials. So the effort to adjust T_N of the AFM materials is interesting and meaningful. In recent years, much attention has been paid to diamagnet diluted face-centered cubic solid solution systems, such as Mg–Co–O systems [6–9], Zn–Co–O systems [10], Mg–Ni–O systems [7,9,11], Zn–Ni–O systems [12] and Li–Ni–O systems [13], in all of which monotonous concentration dependence of T_N were observed. And percolation effects were observed in the Mg–Co–O and Mg–Ni–O systems.

Among all of the AFM materials, Cr_2O_3 is one of the most important AFM 3d transition metal oxides and possesses a T_N of about 307 K. Recently, Cr_2O_3 based systems have attracted much attention in the study of exchange bias effect [14–16]. Most of the works were based on Cr_2O_3 nanoparticles [14–16], and little attention was paid to the magnetic properties of Cr_2O_3 based solid solutions system [17–19]. Though high temperature magnetic properties of $(Al_2O_3)_x(Cr_2O_3)_{1-x}$ solid solutions were investigated [20], this system still lacks systematic study on the magnetic properties. As is known to all, both of Al_2O_3 and Cr_2O_3 are corundum structural with the space group R-3c and the differences between their lattice constants are <4%. So Al_2O_3 and Cr_2O_3 may be mixed in atomic level and form high-quality solid solutions of $(Al_2O_3)_x(Cr_2O_3)_{1-x}$ in the entire range from $x=0$ to $x=1$. It provides us an ideal system to study the doping effect on the magnetic properties of the AFM materials. In the present work, we report the preparation, crystal structure studies and magnetic properties of $(Al_2O_3)_x(Cr_2O_3)_{1-x}$ solid solutions.

2. Experimental

Solid solution samples $(Al_2O_3)_x(Cr_2O_3)_{1-x}$ ($x=0$, 0.1, 0.2, ..., 1.0) were synthesized from pure Al_2O_3 and Cr_2O_3 powders via traditional ceramic production method. The typical procedure is as follows: stoichiometric amounts of Al_2O_3 and Cr_2O_3 powders were mixed together and ground for half an hour in an agate mortar. Then the mixtures were pressed into disks with the diameter of 10 mm. All the as-prepared disks were sintered together to avoid the effect brought by different synthetic processes. After being sintered at 1673 K in air for 10 h, all the samples were ground into powders for phase determination and magnetic studies.

The crystal structures of the products were characterized by X-ray diffraction (XRD, X'pert Philips) with Cu K_α radiation and all the lattice constants were obtained by Rietveld refinement method. The morphology and grain size of the samples were investigated by scanning electron microscopy (SEM, Hitachi-S-3400-N II). Both magnetic hysteresis loops and temperature dependence of magnetization of the samples were performed on a superconducting quantum interference device (SQUID, Quantum Design MPMS XL-7).

* Corresponding author. Tel.: +86 25 83597483; fax: +86 25 83595539.
E-mail address: sgyang@nju.edu.cn (S.G. Yang).

0925-8388/$ – see front matter © 2011 Elsevier B.V. All rights reserved.
doi:10.1016/j.jallcom.2011.04.008

3. Results and discussion

Pure Cr_2O_3 and Al_2O_3 are both rhomb-centered hexagonal structural with the lattice constants of $a = 4.912$ Å, $c = 13.46$ Å (JCPDS NO. 84-0315) and $a = 4.758$ Å, $c = 12.99$ Å (JCPDS NO. 10-0173) respectively. Though the differences between the corresponding lattice constants a and c are both <4%, there is a miscibility gap in this system, and the critical point is located at 30.5 mol% Cr_2O_3 and 1544 K [21]. However one can expect full miscibility by using higher synthesis temperature. In the present work, the synthesis temperature was 1673 K (higher than 1544 K), and we have obtained continuous solid solutions of $(Al_2O_3)_x(Cr_2O_3)_{1-x}$ in the whole range from $x = 0$ to 1, which can be confirmed by XRD and magnetic results in our experiments.

Fig. 1(a) shows the continuous Al–Cr–O solid solutions without any secondary phases for all the samples. As the ionic radius of Cr^{3+} (0.615 Å) is larger than that of Al^{3+} (0.535 Å) [22], the corresponding peaks of the samples shift from lower angles to higher angles with increasing x, which indicates the substitution between Cr^{3+} and Al^{3+} and the formation of the continuous solid solutions in the reaction. Rietveld refinement analysis indicates that the XRD patterns of all the samples can be well fitted using rhomb-centered structure with space group R-3c. The lattice constants a and c calculated from Rietveld refinement versus Al concentration x are plotted in Fig. 1(b), which shows that both lattice constants depend linearly on x. The Vegard's law works well in this case, which is consistent with the results reported in the case of Fe_2O_3–Cr_2O_3 systems [17] and further illustrate the formation of solid solutions.

SEM was used to investigate the morphology and grain size of the as-prepared samples. Fig. 2 shows the typical SEM images. The samples are composed of irregular grains with diameter of 1 μm to several micrometers. The grain size was diminished with the addition of Al ions (Fig. 2(b)–(d)), but it was not further diminished with increasing Al concentration. However, the smallest grain size was several hundred nanometers and most grains were several micrometers. Thus the magnetic properties of all the samples would not be influenced by nano effects.

Magnetic measurements were performed on a SQUID. Zero field cooled temperature dependences of magnetization of all the sam-

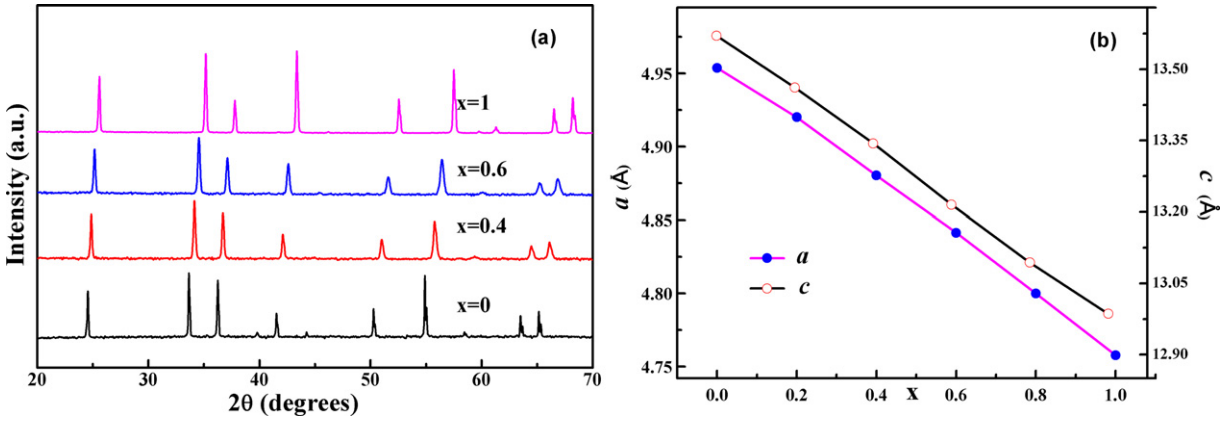

Fig. 1. XRD results of typical $(Al_2O_3)_x$–$(Cr_2O_3)_{1-x}$ samples (a) typical XRD patterns (b) x dependence of lattice constants calculated from Rietveld refinement.

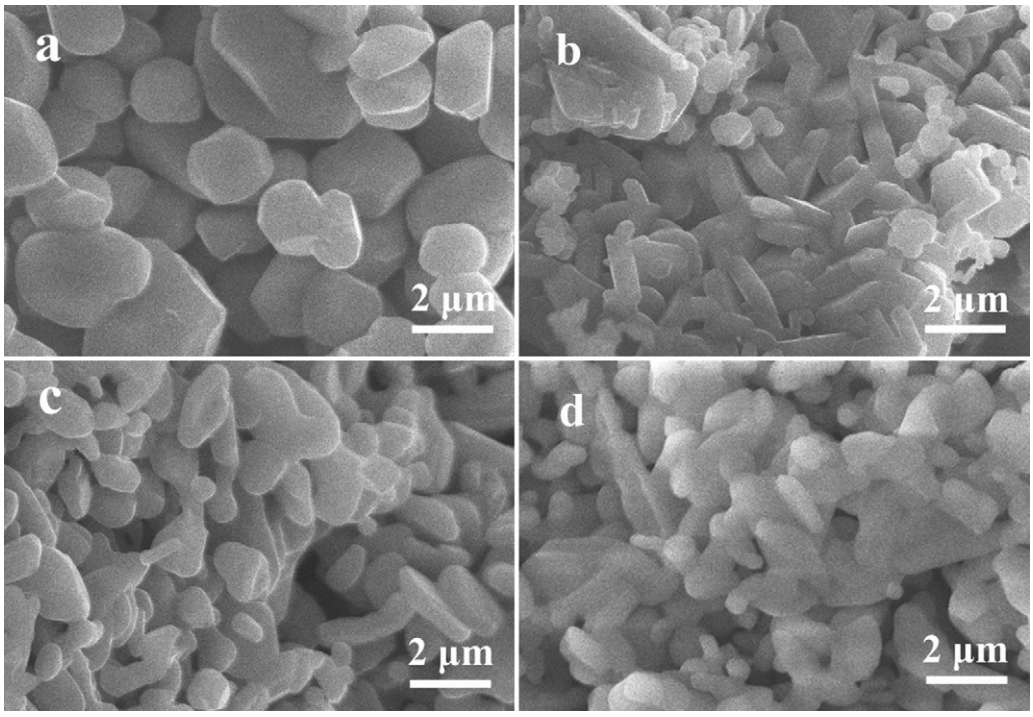

Fig. 2. SEM images of typical $(Al_2O_3)_x$–$(Cr_2O_3)_{1-x}$ samples (a) $x = 0$, (b) $x = 0.4$, (c) $x = 0.6$ and (d) $x = 0.9$.

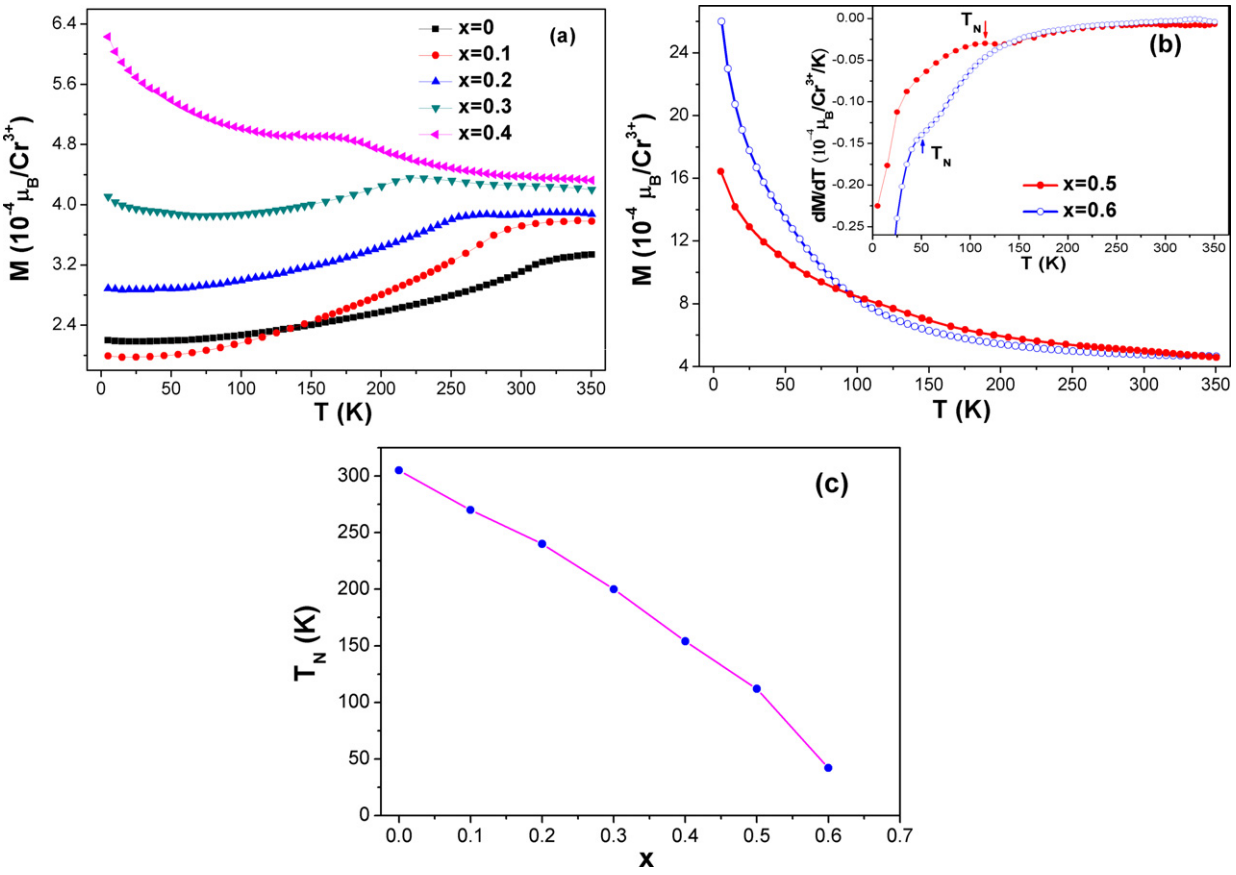

Fig. 3. Zero field cooled temperature dependence of magnetization of the $(Al_2O_3)_x$–$(Cr_2O_3)_{1-x}$ samples with the applied field of 1000 Oe (a) $x = 0$, 0.1, 0.2, 0.3, 0.4 (b) $x = 0.5$, 0.6, inset is the plot of differentiation of M–T results for the two samples and (c) x dependence of T_N of the samples $x = 0$, 0.1, 0.2, . . ., 0.6.

ples were performed in the range from 5 K to 350 K with the applied field of 1000 Oe. Fig. 3(a) shows the results of the samples $x = 0$, 0.1, 0.2, 0.3 and 0.4. The magnetization was normalized in units per Cr^{3+}. Similarly to pure Cr_2O_3, there is a clear peak on every M–T curve which indicates the critical temperature of the corresponding sample. There is only one critical temperature on every M–T curve, which means there is only one transition temperature for one sample. This further illustrates the formation of pure phase solid solutions which is consistent with XRD results. T_N are determined by the maximum value of $\partial M(T)/\partial T$. These values are a few percentage points lower than the position of the peaks in M versus T. These critical temperatures reveal the transition between AFM and PM state. Fig. 3(b) shows the results of the samples $x = 0.5$ and 0.6, there are no very clear peaks in these two curves. The inset of Fig. 3(b) is the temperature dependence of $\partial M(T)/\partial T$ for the two samples, their T_N are obtained by the maximum value of the plots (arrows show the position of T_N). Fig. 3(c) shows the Al_2O_3 concentration x dependence of T_N which gives us almost linear relationship with x below 0.5 and quicker decrease from $x = 0.5$ to 0.6. The decrease of the transition temperature is similar to the results observed in other systems [6–13,23,24]. As Al_2O_3 is diamagnetic and there is no 3d electron for all the Al ions, there is no super exchange interaction between Al and Cr ions. When Al atoms are doped into Cr_2O_3 matrix, the AFM exchange interaction of the crystal is weakened and a lower T_N is observed. As more Al atoms are doped into Cr_2O_3 matrix, the AFM exchange interaction of the crystal grows weaker consequently, which leads to a monotonous decrease of T_N.

When the Al_2O_3 concentration grows higher than 0.6, quite different magnetic properties are observed. Fig. 4 shows the magnetic measurement results of the samples with $x = 0.7$, 0.8 and 0.9. Fig. 4(a) shows the zero field cooled temperature dependence of magnetization of the three samples with the applied field of 1000 Oe. No transition from AFM to PM can be observed on the M–T curves and the temperature dependence of $\partial M(T)/\partial T$ curves. The magnetization of all three samples increases rapidly as the temperature decreases from 50 K to 5 K, which may suggest weak FM behavior in these samples. This result is similar to the results reported in $BiFeO_3$ [25] and Al doped Co–Cu_2O [26] samples. Field dependences of magnetization at 5 K are shown in Fig. 4(b) for the three samples. The presence of hysteresis with coercivity of 15–25 Oe further confirms the existence of the weak FM in these three samples.

Four results should be addressed: for the samples with x smaller than 0.4 very clear transition from AFM to PM can be observed on the M–T curves, while for the samples with x larger than 0.7 weak FM behavior can be observed on the M–H and M–T measurements; for the samples with $x = 0.5$ and 0.6, the transition from AFM to PM becomes indistinct, and a quicker drop of the transition temperatures is observed. All of these results suggest that percolation phenomenon may occur at a concentration between $x = 0.6$ and 0.7. The percolation phenomenon has been observed in Mg–Co–O and Mg–Ni–O solid solutions reported earlier [11,27]. From the extrapolation of the plot of T_N versus Al_2O_3 concentration x, the percolation threshold of the Al–Cr–O solid solution is estimated to be about $x = 0.65$. This percolation effect is reasonable and can be understood as follows: in low Al_2O_3 concentration, the main body of the solid solution is Cr_2O_3 and the long range AFM order in Cr_2O_3 crystal still exist. The doping of Al atoms dilutes the concentration of Cr ions, thus the AFM interaction between Cr atoms becomes weaker with increasing Al_2O_3 concentration, which results in the decrease of critical temperature T_N.

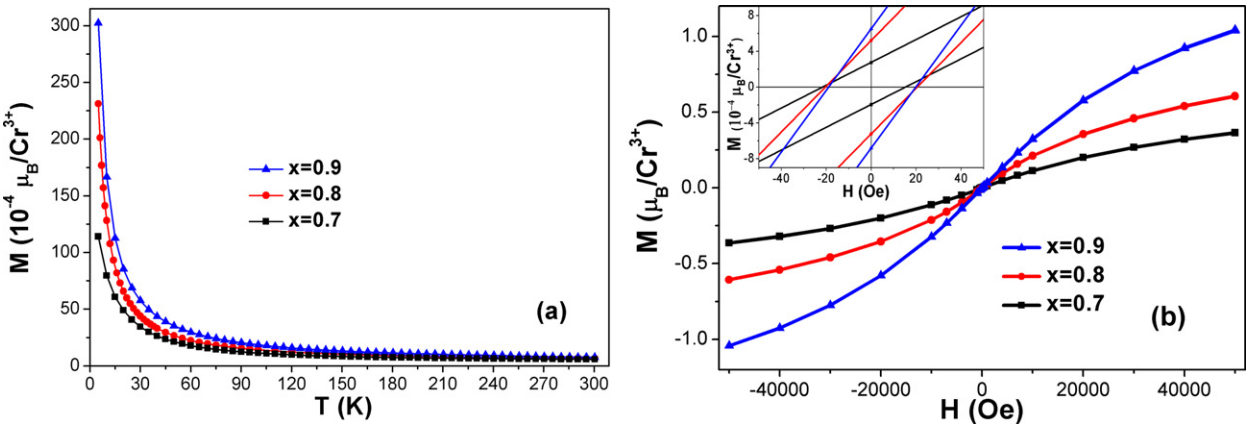

Fig. 4. (a) Zero field cooled temperature dependence of magnetization in the temperature range from 5 K to 300 K with the applied field of 1000 Oe and (b) field dependence of magnetization at 5 K of the samples $x = 0.7$, 0.8 and 0.9, inset is low field range results.

Meanwhile, the magnetization normalized in units per Cr^{3+} becomes higher with increasing Al concentration in the low temperature range except for the sample $x = 0.1$ below 150 K as shown in the M–T curves (see Fig. 3(a)). And the magnetization of all the samples tended to be the same value (lowest $\sim 3.3 \times 10^{-4}\ \mu_B/Cr^{3+}$ and highest $\sim 7.5 \times 10^{-4}\ \mu_B/Cr^{3+}$, the value became higher with increasing x). The different behavior in low temperature range of sample $x = 0.1$ may be due to some uncertain defects in it. The higher magnetization may come from the uncompensated spins due to Cr ions replaced with Al ions. As Al concentration increased, more spins became uncompensated and a higher magnetization was observed. When the Al concentration became high enough, the long range AFM interaction between Cr ions would be destroyed, and weak FM emerged. However, the coupling mechanism of the FM behavior observed at low Cr content is not clear. To understand the mechanism, further experimental and theoretical investigations are needed, by paying attention to the extent of Cr–Cr interactions and to the possible roles of defects in the magnetic behavior.

4. Summary

To sum up, we have synthesized $(Al_2O_3)_x(Cr_2O_3)_{1-x}$ solid solutions in the entire range from $x = 0$ to $x = 1.0$. XRD results showed that all the samples were well crystallized and linear variations of lattice constants a and c were obtained by Rietveld refinement analysis. T_N depended almost linearly on x in the range from $x = 0$ to $x = 0.5$ and decreased more quickly in the range from $x = 0.5$ to 0.6. As x increased to higher than $x = 0.7$, the samples showed weak FM behavior. These facts suggest the percolation effect of the solid solutions with threshold estimated to be about $x = 0.65$. We attributed this behavior to the rupture of the long range AFM order in Al doped Cr_2O_3. FM behavior of the samples with $x = 0.7$, 0.8, 0.9 was observed. However the coupling mechanism at low Cr content is left unclear.

Acknowledgements

This work was supported by the National Natural Science Foundation of China (10774068) and Award for New Century Excellent Talents in University (07-0430).

References

[1] M.N. Baibich, J.M. Broto, A. Fert, F.N. Vandau, F. Petroff, P. Eitenne, G. Creuzet, A. Friederich, J. Chazelas, Phys. Rev. Lett. 61 (1988) 2472–2475.
[2] V. Skumryev, S. Stoyanov, Y. Zhang, G. Hadjipanayis, D. Givord, J. Nogues, Nature 423 (2003) 850–853.
[3] J. Nogues, D. Lederman, T.J. Moran, I.K. Schuller, Phys. Rev. Lett. 76 (1996) 4624–4627.
[4] J. Nogues, J. Sort, V. Langlais, V. Skumryev, S. Surinach, J.S. Munoz, M.D. Baro, Phys. Rep. 422 (2005) 65–117.
[5] W.H. Meiklejohn, C.P. Bean, Phys. Rev. 102 (1956) 1413–1414.
[6] M.S. Seehra, J.C. Dean, R. Kannan, Phys. Rev. B 37 (1988) 5864–5865.
[7] M.M. Ibrahim, Z. Feng, J.C. Dean, M.S. Seehra, J. Phys.: Condens. Matter 4 (1992) 7127–7134.
[8] M.S. Seehra, R. Kannan, M.M. Ibrahim, J. Appl. Phys. 73 (1993) 5468–5470.
[9] R. Masrour, M. Hamedoun, A. Benyoussef, Phys. Lett. A 373 (2009) 3395–3397.
[10] D. Markovic, V. Kusigerski, V. Spasojevic, J. Blanusa, R. Tellgren, Phys. Status Solidi A 201 (2004) 2986–2994.
[11] Z. Feng, M.S. Seehra, Phys. Rev. B 45 (1992) 2184–2189.
[12] D. Rodic, V. Spasojevic, V. Kusigerski, R. Tellgren, H. Rundlof, Phys. Status Solidi B 218 (2000) 527–536.
[13] A.Z. Men'shikov, Y.A. Dorofeev, A.E. Teplykh, B.A. Gizhevskii, N.A. Mironova, Phys. Solid State 42 (2000) 315–320.
[14] S.R. Mishra, I. Dubenko, J. Griffis, N. Ali, K. Marasinghe, J. Alloys Compd. 485 (2009) 667–671.
[15] X.H. Liu, W.B. Cui, X.K. Lv, W. Liu, X.G. Zhao, D. Li, Z.D. Zhang, J. Phys. D: Appl. Phys. 41 (2008) 105005.
[16] D. Tobia, E.L. Winkler, R.D. Zysler, M. Granada, H.E. Troiani, J. Alloys Compd. 495 (2010) 520–523.
[17] T. Grygar, P. Bezdicka, J. Dedecek, E. Petrovsky, O. Schneeweiss, Ceram. Silik. 47 (2003) 32–39.
[18] S. Benny, R. Grau-Crespo, N.H. de Leeuw, Phys. Chem. Chem. Phys. 11 (2009) 808–815.
[19] V. Biondo, S.N. de Medeiros, A. Paesano, L. Ghivelder, B. Hallouche, J.B.M. da Cunha, Solid State Sci. 11 (2009) 1444–1450.
[20] F.S. Stone, J.C. Vickerma, Trans. Faraday Soc. 67 (1971) 316–328.
[21] S.S. Kim, T.H. Sanders, J. Am. Ceram. Soc. 84 (2001) 1881–1884.
[22] R.D. Shannon, C.T. Prewitt, Acta Cryst. B B25 (1969) 925–946.
[23] M.S. Seehra, T.M. Giebultowicz, Phys. Rev. B 38 (1988) 11898–11900.
[24] A.Z. Menshikov, Y.A. Dorofeev, N.A. Mironova, M.V. Medvedev, Solid State Commun. 98 (1996) 839–842.
[25] F. Chen, Q.F. Zhang, J.H. Li, Y.J. Qi, C.J. Lu, X.B. Chen, X.M. Ren, Y. Zhao, Appl. Phys. Lett. 89 (2006) 092910.
[26] S.N. Kale, S.B. Ogale, S.R. Shinde, M. Sahasrabuddhe, V.N. Kulkarni, R.L. Greene, T. Venkatesan, Appl. Phys. Lett. 82 (2003) 2100–2102.
[27] R. Kannan, M.S. Seehra, Phys. Rev. B 35 (1987) 6847–6853.